Clar Sextet Analysis of Triangular, Rectangular and Honeycomb Graphene Antidot Lattices

René Petersen,[†] Thomas Garm Pedersen,[*,†] and Antti-Pekka Jauho[‡,¶]

Department of Physics and Nanotechnology, Aalborg University, DK-9220 Aalborg East, Denmark, Department of Micro- and Nanotechnology, Technical University of Denmark, DTU Nanotech, Building 345 East, DK-2800 Kongens Lyngby, Denmark, and Department of Applied Physics, Aalto University, P. O. Box 11100, FI-00076 AALTO, Finland

E-mail: tgp@nano.aau.dk

Abstract

Pristine graphene is a semimetal and thus does not have a band gap. By making a nanometer scale periodic array of holes in the graphene sheet a band gap may form; the size of the gap is controllable by adjusting the parameters of the lattice. The hole diameter, hole geometry, lattice geometry and the separation of the holes are parameters that all play an important role in determining the size of the band gap, which, for technological applications, should be at least of the order of tenths of an eV. We investigate four different hole configurations: the rectangular, the triangular, the rotated triangular and the honeycomb lattice. It is found that the lattice geometry plays a crucial role for size of the band gap: the triangular arrangement displays always a sizable gap, while for the other types only particular hole separations lead to a large gap. This observation is explained using Clar sextet theory, and we find that a sufficient

---

[*]To whom correspondence should be addressed
[†]Department of Physics and Nanotechnology, Aalborg University, DK-9220 Aalborg East, Denmark
[‡]Department of Micro- and Nanotechnology, Technical University of Denmark, DTU Nanotech, Building 345 East, DK-2800 Kongens Lyngby, Denmark
[¶]Department of Applied Physics, Aalto University, P. O. Box 11100, FI-00076 AALTO, Finland

condition for a large gap is that the number of sextets exceeds one third of the total number of hexagons in the unit cell. Furthermore, we investigate non-isosceles triangular structures to probe the sensitivity of the gap in triangular lattices to small changes in geometry.

keywords graphene, antidots, Clar sextets, band structure, band gap

Graphene, a one atom thick layer of carbon, has attracted a great deal of attention since its discovery in 2004.[1] This is due to its intriguing properties such as extremely high conductivity,[2] high mechanical strength[3] and the ability to probe relativistic phenomena at sub-light speeds.[4] Due to the large conductivity and the atomic layer thickness, graphene is a promising candidate as a substitute for the present principal component of most semiconductor devices, silicon. Natural graphene, however, is a semimetal and thus lacks a band gap which is a necessary condition for its usage in transistor architectures.[4] Introducing a band gap into graphene can be achieved by various means and several approaches have been suggested. For example, slicing graphene into graphene nanoribbons[5] or growing graphene epitaxially on a substrate opens up a band gap in graphene.[6]

Recently however, another approach to opening up a gap in graphene has been suggested. Calculations[7–13] show that by making a triangular array of holes in the graphene layer a band gap is obtained and the size of the gap can be tuned by varying the parameters of the lattice, *i.e.*, the lattice geometry, the hole size and the hole separation. Several recent theoretical articles have explored various aspects of graphene antidot lattices, *e.g.*, electron-phonon coupling,[14,15] detection of edge states,[16] or details of band gap scaling.[17,18] Graphene antidot lattices have also been subject to recent experimental research and antidot lattices of various geometries have been fabricated using a number of different techniques.[12,19–22]

In earlier work triangular antidot lattices have been treated in detail,[7–11,13] and it was found that the size of the band gap is directly linked to the size of the hole compared to the size of the unit cell: the larger the hole the larger the band gap. To make a thorough analysis, one must consider other lattice geometries as well in order to assess whether other geometries might be suited for the actual production of graphene antidot lattices, and also to determine how sensitive the lattices are to small structural variations. Indeed, graphene antidot lattices produced by lithography[19] and

block co-polymer masks[20] will be subject to some uncontrollable variations in the lattice and thus it is important to examine how large an effect these variations may have.
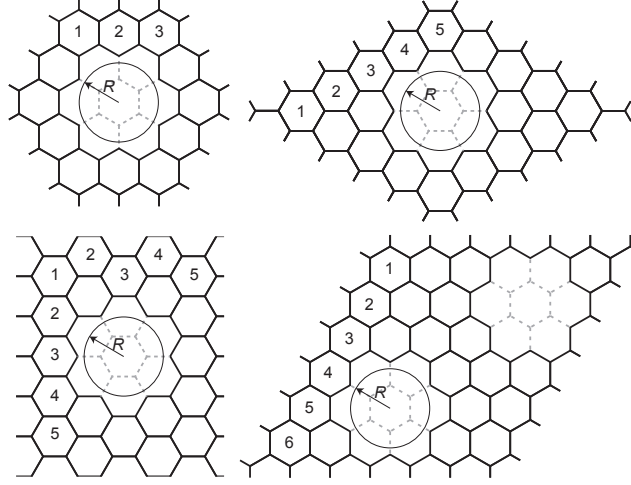

Figure 1: Unit cells of the four types of geometries studied in this paper. Upper left (UL): {3,1} triangular lattice, UR: {5,1} rotated triangular lattice, LL: {5,5,1} rectangular lattice, LR: {6,1} honeycomb lattice. Note that the graphene sheet is rotated 90° in the UL and LR illustration. The numbering in each unit cell shows the non-shared hexagons defining the lattices.

This paper is structured as follows. In Sect. II we introduce the four different lattices we study, as well as the important concept of Clar sextets. Sect. III discusses some computational details, while in Sect. IV we give our main results, and their analysis. Finally, a short conclusion is given in Sect. V.

Antidot lattice geometries

We consider four different lattice types: the triangular lattice, the rotated triangular lattice, the rectangular lattice and the honeycomb lattice. In the following, R is always the radius of the hole given in units of the graphene lattice constant $a_0 = 2.46\text{Å}$.

Triangular. The holes are oriented in a triangular geometry and the unit cell is denoted as $\{L, R\}$ where L is the number of non-shared (belonging to only a single unit cell) hexagons on the edge of the unit cell. This is illustrated in the upper left part of [figure][1][]1 where a {3,1} unit cell is

shown. The numbering in the figure shows the 3 non-shared hexagons. In these geometries, the elementary antidot lattice vectors are parallel to the carbon-carbon bonds.

Rotated triangular. The holes are oriented as in the triangular geometry but rotated $30°$. The unit cell is denoted as $\{L, R\}$ where L is the number of non-shared hexagons on the edge of the unit cell. This is illustrated in the upper right part of [figure][1][]1 where a $\{5,1\}$ unit cell is shown. The elementary antidot lattice vectors are rotated $30°$ with respect to the carbon-carbon bonds.

Rectangular. The holes are located on the corners of a rectangle. The unit cell in this geometry is denoted by $\{L_x, L_y, R\}$ where L_x is the number of non-shared horizontal hexagons and L_y the number of non-shared vertical hexagons in the unit cell. Hence, L_x must be odd to keep the unit cell strictly rectangular. This geometry is illustrated in the lower left part of [figure][1][]1 for a $\{5,5,1\}$ lattice.

Honeycomb. The holes are placed such that they form a honeycomb lattice similar to that of the carbon atoms in a graphene sheet. The unit cell in this geometry is denoted by $\{L, R\}$ where L is the number of non-shared hexagons on the edge of the unit cell. A $\{6,1\}$ unit cell is shown in the lower right part of [figure][1][]1. The centre to centre distance between the holes should be $(L+1)a_0/\sqrt{3}$ and the vector between the holes should be at an angle of $30°$ relative to the zig-zag direction of the graphene sheet for the holes to form a honeycomb lattice. If the first hole is placed such that the centre is exactly in the middle of a hexagon it will not always be such that the centre of the second hole, when placed according to the prescriptions above, is also in the middle of a hexagon. This might cause the holes to be non-similar with respect to the edge of the holes. It turns out that only for unit cells obeying $L = 3n + 2$ (with n an integer) two similar holes can be placed according to the above prescriptions. For the rest, one of the holes must be displaced slightly to make sure that the centre of both holes is in the middle of a hexagon, thereby ensuring that the two holes are similar. The non-perfect honeycomb lattices differ from the other lattices by their reduced symmetry of the unit cell. Thus, one should be careful when calculating band structures

because the irreducible Brillouin zone is larger than for the other geometries.

The selection of structures mentioned above is motivated by recent experimental work. Honeycomb lattices have been produced by patterned hydrogen adsorption,[12] rectangular lattices have been produced using lithography,[19] triangular lattices have been produced using block copolymer methods[20,22] and rotated triangular structures have been produced using a method based on surface-assisted coupling of designed molecular building blocks in Ref.[21] The fact that "'hypothetical"' structures are studied experimentally emphasizes the need for theoretical investigations to guide the experimental work and possibly the fabrication of devices based on graphene antidot lattices.

To examine the structures we will calculate band structures of the lattices and analyze their Clar structure, that is, the pattern of delocalized π-orbital phenyl ring structures, *i.e.* Clar sextets.[23] Clar analysis has previously been used with success to explain the oscillating behaviour of the band gap in graphene nanoribbons,[24] and the stability and band gap of carbon nanotubes.[25] Very recently, we gave a preliminary discussion of lattice-dependence of band gaps in rectangular graphene antidot lattices.[26] The Clar structure of a given unit cell of a lattice is determined by locating the pattern of sextets, which gives the maximum number of sextets in the unit cell. The sextets cannot be distributed freely within the unit cell due to two limitations: The Clar representation has to preserve the unit cell (if it failed to do so, it would not, by definition, be a unit cell) and two sextets cannot be neighbors. Neighboring sextets are non-chemical since they would require carbon atoms with more than four bonds. In most cases it is straightforward to determine the Clar structure while in others it is more involved due to lack of symmetry. In those cases we have calculated the bond order to aid in finding the optimal Clar structure. Here it should be noted that in many cases the Clar structure is not unique. For many structures several different Clar structures yield the same total number of sextets. Thus, when calculating the bond order one will find a superposition of all the distinct Clar structures. This is not crucial, because, as it will be explained below, what really matters for our purpose is the number of sextets.

Results and discussion

The results of the band structure calculations of the NN-TB model are shown in [figure][2][]2-[figure][5][]5. [figure][2][]2 shows the band structure of three triangular antidot lattices differing in the unit cell size, that is, the separation between the holes. As shown previously[7,8] triangular antidot lattices show a band gap for all tested configurations and the band gap E_g is proportional to the ratio between the number of atoms removed to form the hole and the total number of atoms in the unit cell before the hole is formed: $E_g \propto N_{\text{removed}}^{1/2}/N_{\text{total}}$.[7,8] To illustrate the fact that the band gap simply decreases monotonously with unit cell size for a fixed hole, we have considered {5,1}, {6,1} and {7,1} triangular lattices. As clearly observed in [figure][2][]2, all the chosen structures have large band gaps and the band gap is always located at the Γ point of the Brillouin zone. Indeed, it is observed that the band gap decreases as the ratio between the hole size and unit cell size decreases, that is, as the ratio $N_{\text{removed}}^{1/2}/N_{\text{total}}$ decreases.

The story is different for other geometries, as demonstrated by [figure][3][]3, which gives the band structures for the rotated triangular lattices. No band gap is observed for the structures {4,1} and {6,1} and around the K point the bands resemble the bands of pristine graphene: no gap is observed and the bands are linear in the proximity of the K point. As we shall discuss below, for general structures of the type {L,R} only every third value of L leads to a substantial band gap.

When analyzing the band structures of rectangular and honeycomb/near-honeycomb (because the lattice is disrupted to make the holes similar) antidot lattices the picture is similar to the rotated triangular lattices. For the three rectangular lattices shown in [figure][4][]4 all structures have a finite band gap but only {7,8,2} presents a large band gap, while {7,9,2} and {7,10,2} have significantly smaller band gaps. For the three honeycomb lattices in [figure][5][]5 only {5,1} presents a large gap. These findings strongly suggest that some connection should exist between certain general characteristics of the lattice and the appearance of a large band gap. It should be pointed out that the band gap is not exactly zero for any of the shown structures but it is indeed very small in magnitude (on the order of few meV).

To explain the presence of a large band gap for certain structures and the lack of a band gap
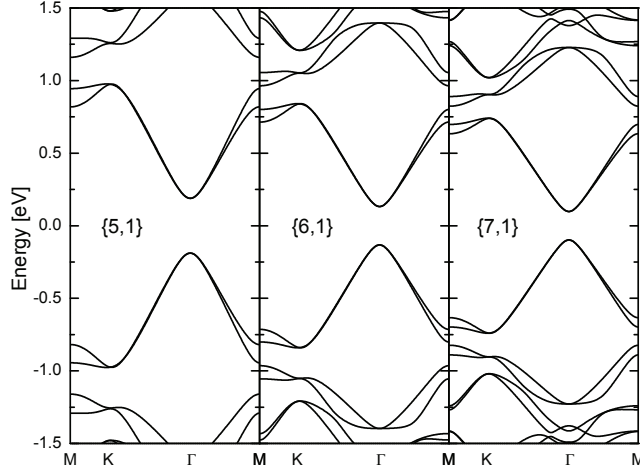
Figure 2: Band structure of the triangular antidot lattices {5,1}, {6,1} and {7,1}. A band gap is present for all structures and it is always located at the Γ point of the Brillouin zone.

for other structures we suggest that one should analyze the Clar representation of the unit cell. By doing this one finds that not all of the structures support a complete benzenoid pattern because the Clar sextets cannot be distributed freely across the unit cell. The Clar representation of the triangular lattice is particularly simple because it always allows for a complete benzenoid structure just like in pristine graphene. In other words, the introduction of the holes does not disturb the structure of the resonant double bonds and thus the resonant structure remains the same as in pristine graphene. The only exception to this rule is related to the double bonds around the hole which, depending on the radius of the hole, may not be allowed to maintain their chemical structure. [figure][6][]6 shows the Clar structure of two unit cells belonging to the triangular lattice, {3,1} and {4,1}. Both structures support the complete benzenoid pattern. According to Clar sextet theory[24]
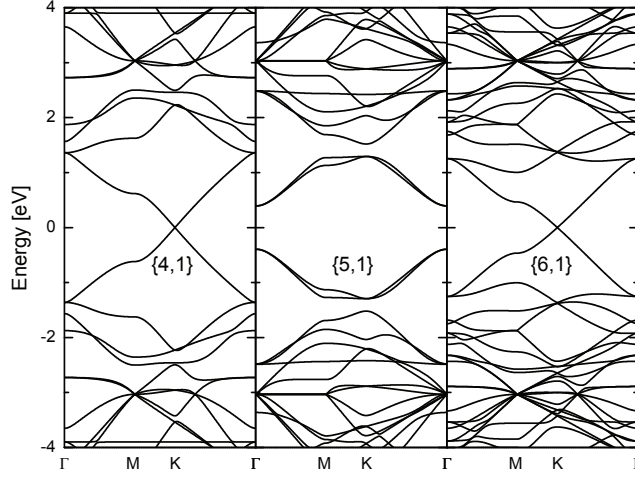
7

Figure 3: Band structure of the rotated triangular structures {4,1}, {5,1} and {6,1}. Only one of the structures shown possesses a band gap while the others resemble the behaviour of intact graphene near the *K* point.

fully benzenoid structures have higher stability than structures for which a fully benzenoid bonding pattern is not possible. Thus, one can expect triangular lattices to be more stable than other geometries.

For the other lattice types a complete benzenoid pattern is not always a possibility. This becomes evident by studying [figure][7][]7-[figure][9][]9. From these figures one can also see that the 3-periodic patterns found for the band gaps are replicated in the Clar patterns of the structures. Thus, only those structures, which have a fully benzenoid pattern lead to a large band gap while the other structures either present a gap that is significantly smaller (for the rectangular lattices a reduction of a factor 5 is seen) or practically zero. By combining the calculations of the band structures with the Clar representations of the unit cells we may deduce a set of semi-empirical
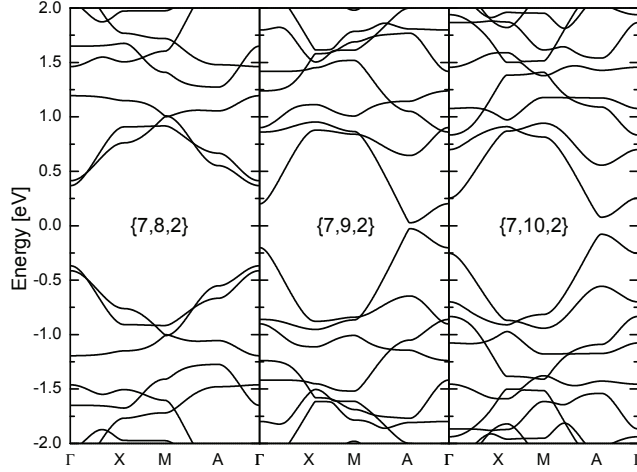
Figure 4: Band structure of the rectangular lattice structures {7,8,2}, {7,9,2} and {7,10,2}. Only one of the structures shown possesses a band gap while the others resemble the behaviour of intact graphene.

rules for the occurrence of a large band gap; these rules are summarized in the Table 1. Thus, the structures with significant band gaps constitute only one third of the total number of structures within these last three classes of lattices. These findings are based on the NN-TB model but we have replicated the same patterns in the QT-TB model in order to verify that the conclusions drawn are not based on artifacts of an oversimplified model.

The possibility of making a complete benzenoid pattern of Clar sextets in graphene antidot lattices, ignoring the disruption of the Clar structure by the hole, seems to be a criterion for the appearance of a large band gap. Evidently, all triangular antidot lattices do possess a band gap and they all support a complete benzenoid pattern of sextets. On the contrary, for the other lattices, only a minority of all structures support a complete benzenoid pattern and consequently possess
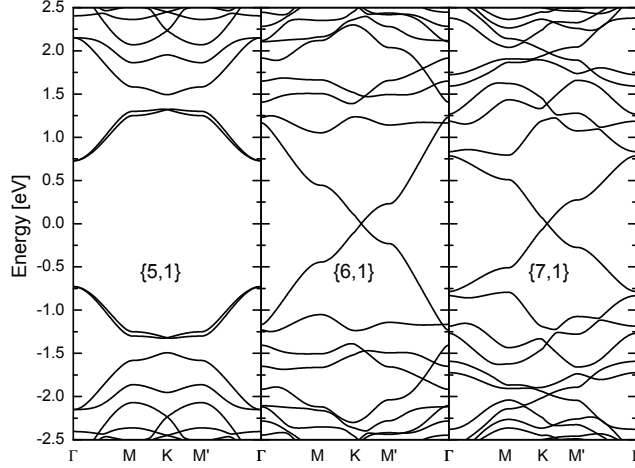
9

Figure 5: Band structure of the honeycomb lattices {5,1}, {6,1} and {7,1}. A band gap is only present for one of the shown structures.

a large band gap. For hole sizes of $R = 1$ it seems that the band gap is either large or close to zero. In order to extend our conclusions to larger (and more realistic) geometries, we have tested a large number of rotated triangular lattices as a function of the hole size $R = 1..7$ and the lattice spacing $L = 5..20$, see [figure][10][]10. We always find that the prediction of the Clar sextet theory holds: as a function of L only every third structure has a sizable gap. The size of the gap always decreases as L is increased; however the quantitative details depend on the value of R, and are thus beyond the qualitative statements that can be deduced from the Clar theory. Moreover, in Ref.[26] we have verified Clar theory for $R = 2$ rectangular lattices. In general, our calculations indicate that a criterion for a large band gap is the existence of a complete benzenoid Clar pattern. In an attempt to find a simple rule for the existence of a large band gap we counted the number of sextets
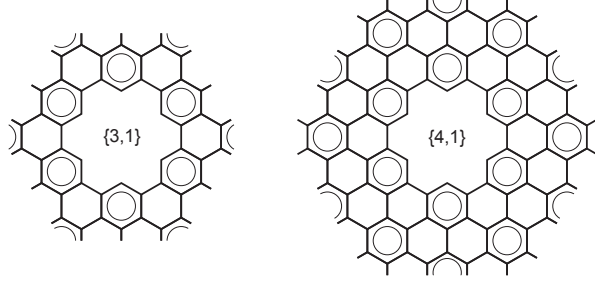
Figure 6: Clar structure of the triangular lattice. Here it is clear that all lattices support a complete benzenoid structure for a hole of radius a_0.
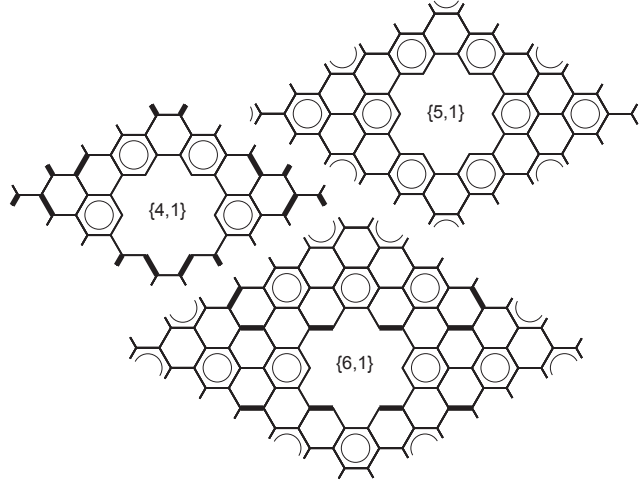

Figure 7: Clar structure of the triangular rotated lattice. As it is seen, a complete benzenoid pattern is not possible for all structures. The hole radius is a_0 in all cases.

in the unit cells and related it to the total number of hexagons in the cell. We found that, for those structures having a large band gap, the number of sextets in the unit cell was larger than one third of the total number of hexagons in the unit cell, $N_{Sx} > \frac{1}{3} N_{Hx}$.

From these findings we conclude that the non-rotated triangular lattice holds the most potential for the actual production of graphene antidot lattice of technological importance, since a band gap is found in all cases. Thus, it is interesting to study the stability of this structure under small geometric distortions. Here we will consider a non-isosceles triangular lattice as shown in [figure][11][]11. All unit cells are effectively elongated in the *y*-direction and the deviation from the triangular case is denoted with the parameter *D*, which expresses how much the vertical distance between the holes is larger than in the triangular case. *D* is measured in units of a_0 and a lattice of
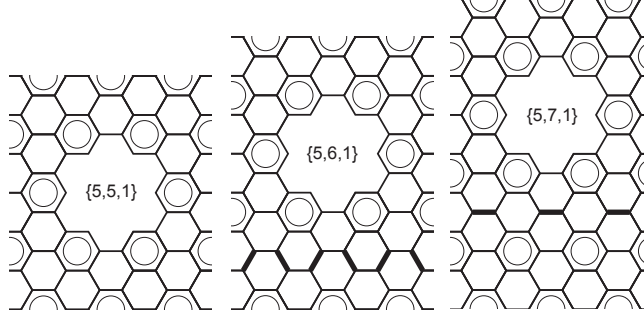
Figure 8: Clar structure of the rectangular lattice. As it is seen, a complete benzenoid pattern is not possible for all structures. The hole radius is a_0 in all cases.
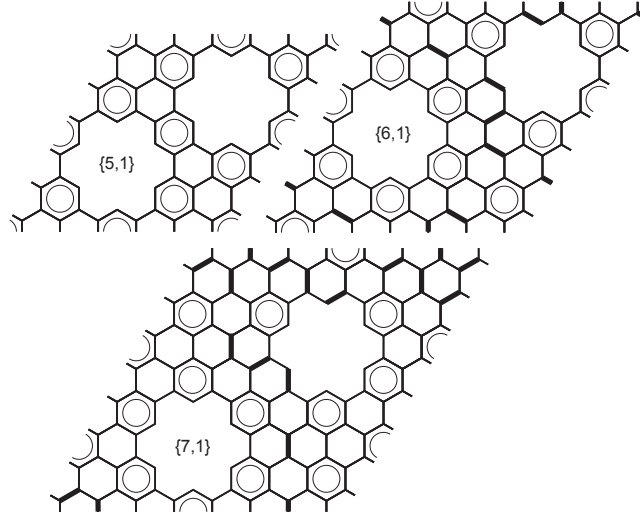
Figure 9: Clar structure of the honeycomb lattice. As it is seen, a complete benzenoid pattern is not possible for all structures. The hole radius is a_0 in all cases.

the non-isosceles triangular type is denoted as $\{L, D, R\}$ where L retains its original meaning. The elongation of the unit cell in the y-direction disturbs the previously complete benzenoid structure and one could suspect that a similar three fold repetitive pattern as those seen for other types of structures should be seen. Indeed, if one analyzes the Clar pattern it is found that every third structure, those with $D = 3n$, support a complete benzenoid Clar structure. Looking a [table][2][]2 one can see that these structures are exactly those, which also possess a band gap, in accordance with the findings for other structures.

Thus, as a guide to experimental fabrication of large-gap antidot lattices we stress the following points: First, triangular lattices are favorable due to their insensitivity to the precise lattice constant.

Table 1: Empirical rules governing the occurrence of a large band gap. n is a non-negative integer.

Structure	large band gap
triangular	no restrictions
rotated triangular	$L = 3n + 2$
rectangular	$L_y = 3n + 2$
honeycomb	$L = 3n + 2$

Figure 10: Band gaps of $\{L,R\}$ rotated triangular antidot lattices. The R values are indicated next to each data point.

It is essential, however, that the elementary lattice vectors connecting neighboring holes are aligned along the carbon-carbon bonds. Also, it is important to maintain six-fold rotational symmetry as demonstrated by the analysis of non-isosceles lattices. In practice, orientation of the antidot lattice relative to the graphene lattice requires knowledge of the latter. This may be obtained by electron diffraction,[27] transmission electron microscopy[28] or polarized Raman spectroscopy.[29] Controlling the orientation of the lattice should be feasible with lithography[19] but probably challenging with the block copolymer technique.[20] Alternatively, chemical self-assembly from suitable precursors can be applied to ensure a particular lattice geometry.[21]

Figure 11: A non-isosceles triangular lattice. This lattice is denoted by $\{L,D,R\}$ where L and R are the same as in the triangular case and D measure the deviation of the hole shown from its original position in the triangular lattice. D is measured in units of a_0 and can be negative.

Table 2: Band gaps and position of band gaps within the Brillouin zone of non-isosceles triangular structures. Structures which allow for complete benzenoid structures are marked with a star.

Structure	E_g[eV]	Pos $\vec{b}_1$	Pos $\vec{b}_2$
{5,0,1.0}*	0.377	0.000	0.000
{5,1,1.0}	0.044	0.667	0.333
{5,2,1.0}	0.052	0.667	0.333
{5,3,1.0}*	0.269	0.000	0.000
{5,4,1.0}	0.033	0.667	0.333
{5,5,1.0}	0.089	0.667	0.333
{5,6,1.0}*	0.210	0.000	0.000

Conclusion

Our results show that it is possible, without turning to full-scale atomistic calculations, predict if a given graphene antidot structure can be expected to possess a large band gap only by analyzing the Clar structure of the unit cell. Structures investigated in this work show a large band gap only if the lattice allows for a complete benzenoid pattern with the number of sextets exceeding one third of the total number of hexagons in the unit cell. Four different lattice types were investigated. We found that only non-rotated triangular lattices, in which antidot lattice vectors are parallel to atomic bonds, are insensitive to lattice constants and always exhibit a band gap. All other lattices (rotated triangular, rectangular and honeycomb) are extremely sensitive to the lattice geometry and only one third display large band gaps. Finally, non-isosceles triangular lattices show the same three-fold repetitive pattern with respect to the band gap.

Methods

In the present work, band structures of antidot lattices are calculated in a simple nearest neighbor tight binding model (NN-TB) as well as the quasi-particle tight binding (QP-TB) model[8] based on the parametrization of the quasi-particle band structure of graphene.[30] In the NN-TB model the hopping integral between neighbor atoms is given by $\gamma = 3.033\text{eV}$[31] and overlap is neglected. In the QP-TB model the parameters are used as given in Ref.[30] and three nearest neighbors and

overlaps are included in the calculations.

In certain cases, the Clar structure is difficult to identify and for this purpose the bond order (BO) pattern has been examined. In graphene and related structures one can calculate the BO between two bound atoms by calculating the overlap between the π-electrons of the two atoms. This gives information about the probability of finding a double bond between those two atoms. The BO between atom p and p' (neighboring atoms) is calculated as follows

$$BO_{pp'} = \sum_{v}\sum_{v'} (c_v^p)^* c_{v'}^{p'}.$$ (1)

Here, c_v^p is the expansion coefficient of valence band state v in the basis of π-orbitals labeled by their site p, and the sums are taken over all valence band states v, v'. In the present case, this entails a summation over k-points in the irreducible Brillouin zone as well as band index. A large BO is indicative of double-bond character and the BO pattern is therefore helpful in identifying the Clar pattern. We do not explicitly show the obtained BO patterns but merely ensure their agreement with all presented Clar structures.

Acknowledgement

References

1. Novoselov, K. S.; Geim, A. K.; Morozov, S. V.; Jiang, D.; Zhang, Y.; Dubonos, S. V.; Grigorieva, I. V.; Firsov, A. A. Electric Field Effect in Atomically Thin Carbon Film. *Science* **2004**, *306*, 666–669.

2. Du, X.; Skachko, I.; Barker, A.; Andrei, E. Y. Approaching Ballistic Transport in Suspended Graphene. *Nat. Nanotechnol.* **2008**, *3*, 491–495.

3. Lee, C.; Wei, X.; Kysar, J. W.; Hone, J. Measurement of the Elastic Properties and Intrinsic Strength of Monolayer Graphene. *Science* **2008**, *321*, 385–388.

4. Neto, A. H. C.; Guinea, F.; Peres, N. M. R.; Novoselov, K. S.; Geim, A. K. The Electronic Properties of Graphene. *Rev. Mod. Phys.* **2009**, *81*, 109–162.

5. Barone, V.; Hod, O.; Scuseria, G. E. Electronic Structure and Stability of Semiconducting Graphene Nanoribbons. *Nano Lett.* **2006**, *6*, 2748–2754.

6. Zhou, S. Y.; Gweon, G.-H.; Fedorov, A. V.; First, P. N.; Heer, W. A. D.; Lee, D. H.; Guinea, F.; Neto, A. H. C.; Lanzara, A. Substrate-Induced Bandgap Opening in Epitaxial Graphene. *Nat. Mater.* **2007**, *6*, 770–775.

7. Pedersen, T. G.; Flindt, C.; Pedersen, J.; Mortensen, N. A.; Jauho, A.-P.; Pedersen, K. Graphene Antidot Lattices: Designed Defects and Spin Qubits. *Phys. Rev. Lett.* **2008**, *100*, 136804.

8. Petersen, R.; Pedersen, T. G. Quasiparticle Properties of Graphene Antidot Lattices. *Phys. Rev. B* **2009**, *80*, 113404.

9. Pedersen, T. G.; Flindt, C.; Pedersen, J.; Jauho, A. P.; Mortensen, N. A.; Pedersen, K. Optical Properties of Graphene Antidot Lattices. *Phys. Rev. B* **2008**, *77*, 245431.

10. Pedersen, T. G.; Jauho, A.-P.; Pedersen, K. Optical Response and Excitons in Gapped Graphene. *Phys. Rev. B* **2009**, *79*, 113406.

11. Fürst, J. A.; Pedersen, J. G.; Flindt, C.; Mortensen, N. A.; Brandbyge, M.; Pedersen, T. G.; Jauho, A.-P. Electronic Properties of Graphene Antidot Lattices. *New J. Phys.* **2009**, *11*, 095020.

12. Balog, R.; Jørgensen, B.; Nilsson, L.; Andersen, M.; Rienks, E.; Bianchi, M.; Fanetti, M.; Lægsgaard, E.; Baraldi, A.; Lizzit, S. et al. Bandgap Opening in Graphene Induced by Patterned Hydrogen Adsorption. *Nat. Mater.* **2010**, *9*, 315–319.

13. Vanevic, M.; Stojanovic, V. M.; Kindermann, M. Character of Electronic States in Graphene Antidot Lattices: Flat Bands and Spatial Localization. *Phys. Rev. B* **2009**, *80*, 045410.

14. Vukmirovic, N.; Stojanovic, V. M.; Vanevic, M. Electron-Phonon Coupling in Graphene Antidot Lattices: An Indication of Polaronic Behavior. *Phys. Rev. B* **2010**, *81*, 041408(R).

15. Stojanovic, V. M.; Vukmirovic, N.; Bruder, C. Polaronic Signatures and Spectral Properties of Graphene Antidot Lattices. *Phys. Rev. B* **2010**, *82*, 165410.

16. Wimmer, M.; Akhmerov, A. R.; Guinea, F. Robustness of Edge States in Graphene Quantum Dots. *Phys. Rev. B* **2010**, *82*, 045409.

17. Liu, W.; Wang, Z. F.; Shi, Q. W.; Yang, J.; Liu, F. Band-Gap Scaling of Graphene Nanohole Superlattices. *Phys. Rev. B* **2009**, *80*, 233405.

18. Martinazzo, R.; Casolo, S.; Tantardini, G. F. Symmetry-Induced Band-Gap Opening in Graphene Superlattices. *Phys. Rev. B* **2010**, *81*, 245420.

19. Eroms, J.; Weiss, D. Weak Localizations and Transport Gap in Graphene Antidot Lattices. *New. J. Phys.* **2009**, *11*, 095021.

20. Bai, J.; Zhong, X.; Jiang, S.; Huang, Y.; Duan, X. Graphene Nanomesh. *Nat. Nanotechnol.* **2010**, *5*, 190–194.

21. Bieri, M.; Treier, M.; Cai, J.; Aït-Mansour, K.; Ruffieux, P.; Gröning, O.; Gröning, P.; Kastler, M.; Rieger, R.; Feng, X. et al. Porous Graphenes: Two-Dimensional Polymer Synthesis with Atomic Precision. *Chem. Commun.* **2009**, *45*, 6919–6921.

22. Kim, M.; Safron, N. S.; Han, E.; Arnold, M. S.; Gopalan, P. Fabrication and Characterization of Large-Area, Semiconducting Nanoperforated Graphene Materials. *Nano. Lett* **2010**, *10*, 1125–1131.

23. Clar, E. *The Aromatic Sextet*; Wiley, 1972.

24. Baldoni, M.; Sgamellotti, A.; Mercuri, F. Electronic Properties and Stability of Graphene Nanoribbons: An Interpretation based on Clar Sextet Theory. *Chem. Phys. Lett.* **2008**, *464*, 202–207.

25. Baldoni, M.; Sgamellotti, A.; Mercuri, F. Finite-Length Models of Carbon Nanotubes Based on Clar Sextet Theory. *Org. Lett.* **2007**, *9*, 4267–4270.

26. Petersen, R.; Pedersen, T. G.; Jauho, A.-P. Clar Sextets in Square Graphene Antidot Lattices. **2010**, Unpublished.

27. Knox, K. R.; Wang, S.; Morgante, A.; Cvetko, D.; Locatelli, A.; Mentes, T. O.; Niño, M. A.; Kim, P.; Osgood, R. M. Spectromicroscopy of Single and Multilayer Graphene Supported by a Weakly Interacting Substrate. *Phys. Rev. B* **2008**, *78*, 201408.

28. Meyer, J. C.; Geim, A.; Katsnelson, M.; Novoselov, K.; Booth, T.; Roth, S. The Structure of Suspended Graphene Sheets. *Nature* **2007**, *446*, 60–63.

29. Huang, M.; Yan, H.; Chen, C.; Song, D.; Heinz, T. F.; Hone, J. Phonon Softening and Crystallographic Orientation of Strained Graphene Studied by Raman Spectroscopy. *Proc. Nat. Acad. Sci.* **2009**, *106*, 7304–7308.

30. Grüneis, A.; Attaccalite, C.; Wirtz, L.; Shiozawa, H.; Saito, R.; Pichler, T.; Rubio, A. Tight-Binding Description of the Quasiparticle Dispersion of Graphite and Few-Layer Graphene. *Phys. Rev. B* **2008**, *78*, 205425.

31. Saito, R.; Dresselhaus, G.; Dresselhaus, M. S. *Physical Properties of Carbon Nanotubes*; Imperial College Press, 1998

.